Theoretical Study of One- and Two-Photon Absorption Properties of Octupolar D_{2d} and D_3 Bipyridyl Metal Complexes

Xiang-Biao Zhang,[†] Ji-Kang Feng,*[,†,‡] and Ai-Min Ren[†]

State Key Laboratory of Theoretical and Computational Chemistry, Institute of Theoretical Chemistry, JiLin University, Changchun 130023, People's Republic of China, College of Chemistry, JiLin University, Changchun 130023, People's Republic of China

Received: October 21, 2006; In Final Form: December 18, 2006

The molecular equilibrium structures, electronic structures, and one- and two-photon absorption (TPA) properties of C_{2v} (Zn(II), Fe(II) and Cu(I)) dipolar and D_{2d} (Zn(II) and Cu(I)) and D_3 (Zn(II)) octupolar metal complexes featuring different functionalized bipyridyl ligands have been studied by the ZINDO-SOS method. The calculated results show that one- and two-photon absorption properties of metal complexes are strongly influenced by the nature of the ligands (donor end groups and π linkers) and metal ions as well as by the symmetry of the complexes. The length of the π-conjugated backbone, the Lewis acidity of the metal ions, and the increase of ligand-to-metal ratio result in a substantial enhancement of the TPA cross sections of metal complexes. Substitution of C═N and N═N for C═C plays an important role in altering the maximum TPA wavelengths and the maximum TPA cross sections of metal complexes. Of them, the C═N substituted metal complexes have relatively large TPA cross sections. Replacing styryl with thienylvinyl makes the one-photon absorption wavelength red shift and at the same time leads to a great decrease of the maximum TPA cross sections of metal complexes. The possible reason is discussed. In the range 500−1250 nm, octupolar metal complexes exhibit intense TPAs and therefore are promising candidates for TPA materials.

Introduction

Two-photon absorption (TPA) in organic molecules has received considerable attention in recent years, owing to a number of potential applications[1−4] in several areas of biophotonics and material science, such as two-photon up-conversion lasing,[1] optical power limiting,[2] photodynamic therapy,[3] and three-dimensional (3D) microfabrication.[4] The push−pull dipolar molecules, in the earlier studies, have been the active research point, because this kind of molecule generally has large TPA cross sections.[5−10] However, these dipoles may present many problems from a material standpoint, and it is the dipole−dipole electrostatic interactions that often result in an antiparallel molecular arrangement and a subsequent cancellation of the nonlinear response at bulk materials.[11] In addition, the optimized molecular structures for this kind of molecule often lead to a red shift of linear absorption, damaging the transparency of materials.[6−9] To overcome these difficulties, the enlarged potential for nonlinear optics of octupolar molecules[12,13] has sparked intense research in design of excellent TPA materials. Compared with the 1D dipolar TPA chromophores, octupolar molecules possess more round-off shapes, which ease their packing in a single crystalline lattice as opposed to less favorable elongated dipolar rodlike molecules; the absence of dipolar moments in the excited as well as the ground state makes octupolar molecules more suitable in various optical applications.[14−16] More importantly, octupolar compounds resolve the inherent conflict between the transparency and nonlinearity existing in traditional dipolar molecules. The results of experiments and theoretical calculations reveal that the TPA cross section value increases on proceeding from dipolar to octupolar molecules and also with increasing donor and acceptor strength.[17−21] Most octupolar systems developed to date are organic molecules. They have been designed by chemical functionalization of a central core and can be roughly classified into three main classes: (1) 2D or 3D molecules of global D_{3h} and C_3 symmetry obtained by 1,3,5-functionalization of a central aromatic core (phenyl or triazine);[19] (2) D_{3h} or slightly twisted D_3 propeller-like molecules, such as functionalized trivalent carbocation, boron, aluminum, or nitrogen atoms;[20] and (3) 3D tetrahedral molecules, such as tetrasubstituted carbon or phosphonium derivatives.[21a] Other examples of octupolar structures, such as paracyclophane, truxenone, sumanene, and triphenylene derivatives, have also been described recently.[21b−e]

Coordination chemistry has proved to be another powerful tool to build up octupolar arrangements. Metal ions can assemble organic ligands in a variety of multipolar arrangements which show interesting electronic and optical properties tunable by virtue of the coordinated metal center. In the UV−visible region of spectrum of metal complexes, there are often two different transitions, i.e., a strong intraligand charge-transfer (ILCT) transition and a low-energy metal to ligand charge-transfer transition (MLCT), which are often associated with large TPA cross section. High damage threshold and fast response time that metal complexes have in comparison to organic compounds are important from the perspective of application. A wide range of metals with different oxidation states and ligands necessarily make metal complexes an active research point in design of TPA material. Some reports are available describing the effect of metal ions on TPA-active organic molecules. Mg(II) was shown to lower the TPA cross section values by 50% in an azo-crown ether connected to distyrylbenzenes in the donor-π-acceptor-π-donor format.[22] Upon binding with Ni(II) ion, the

* Corresponding author. E-mail address: jikangf@yahoo.com.
† Institute of Theoretical Chemistry, JiLin University.
‡ College of Chemistry, JiLin University.

10.1021/jp0669097 CCC: $37.00
Published on Web 01/26/2007

TPA cross sections of 1,10-phenanthroline-based π-conjugated TPA chromophores increase from 165 GM (1GM = 10^{-50} cm^4s/photon) to 578 GM.[23] Recently, Debabrata, Parimal and coworkers report that complexation of a Schiff base with metal ions (Cu(I) and Zn(II)) induces exceptionally large TPA cross section values (1700 GM to 10736 GM), depending on the structure of the complex.[24] However, to our best knowledge, systematical study on TPA properties of octupolar metal complexes has not been reported in literature. In this paper, we design a series of dipolar and octupolar bipyridyl metal complexes that have been reported to exhibit high quadratic hyperpolarizability[25−29] and systematically study the influence of the nature of ligands and metallic centers as well as symmetry of the complexes on their TPA properties to provide useful physical insights for the same kind of metal complexes.

Computational Methods

The TPA process corresponds to simultaneous absorption of two photons. The TPA efficiency of an organic molecule, at optical frequency $\omega/2\pi$, can be characterized by the TPA cross-section $\delta(\omega)$. It can be directly related to the imaginary part of the second hyperpolarizability $\gamma(-\omega;\omega,\omega,-\omega)$ by refs 30 and 31

$$\delta(\omega) = \frac{3\hbar\omega^2}{2n^2c^2\epsilon_0} L^4 \, \mathrm{Im}[\gamma(-\omega;\omega,-\omega,\omega)] \qquad (1)$$

where $\hbar\omega$ is the energy of the incoming photons, c is the speed of light, and ϵ_0 is the vacuum electric permittivity. n denotes the refractive index of the medium, and L corresponds to the local-field factor. In the calculations presented here, n and L are set to 1 (isolated molecule in vacuum).

The sum-over-state (SOS) expression to evaluate the components of the second hyperpolarizability $\gamma_{\alpha\beta\gamma\delta}$ can be deduced from perturbation theory and density matrix method. By consideration of a power expansion of energy with respect to the applied field, the $\gamma_{\alpha\beta\gamma\delta}$ Cartesian components are given by refs 32 and 33. In the present work, all damping factors Γ are set 0.13 eV. To compare the calculated δ value with experimental value measured in solution, the orientationally averaged (isotropic) value of γ is evaluated, which is defined as

$$\langle\gamma\rangle = \frac{1}{15}\sum_{i,j}(\gamma_{iijj} + \gamma_{ijij} + \gamma_{ijji}) \qquad i,j = x,y,z \qquad (2)$$

Substituting the imaginary part of $\langle\gamma\rangle$ value into (1), a $\delta(\omega)$ value that can be compared with the experimental value is obtained.

In principle, any kind of self-consistent field molecular orbital procedure combined with configuration interaction (CI) can be used to calculate the physical values in the SOS expressions. In this paper, considering the number and size of studied compounds, we first used the DFT/B3LYP/6-31G method to calculate molecular equilibrium geometries. Then the properties of electronic excited states were obtained by single and double electronic excitation configuration interaction (SDCI) using ZINDO program.[34a] For all the molecules, the Mataga-Nishimoto potential was employed to describe long-range Coulomb interactions; the CI-active spaces were restricted to the fifteen highest occupied and the fifteen lowest unoccupied π-orbitals for singly excited configuration and to the three highest occupied and the three lowest unoccupied π-orbitals for doubly excited configuration. Furthermore, one-photon absorption (OPA) parameters that are needed to predict TPA properties were provided. Then according to the (1), (2) and SOS formulas, the second hyperpolarizabilities γ and the TPA cross-sections $\delta(\omega)$ have been calculated. For every molecule, the calculated TPA cross section includes the contributions from 200 lowest-lying excited states.

Results and Discussions

Molecular Design and Optimization. The structures of studied molecules are shown in Figure 1. In this paper, our aims are as follows: (1) To study the effect of the nature of ligands in metal complexes on one- and two-photon absorption properties of metal complexes. The design of the push−pull styryl-bipyridyl ligands terminated by hydrogen (**a**), methyloxy (**b**) and dimethylaimno (**c**) donor groups allows us to assess the effect of donor strengths on one- and two-photon absorption properties of metal complexes. Replacement of the styryl in **c** by phenylimino, phenylazo, thienylvinyl, and bistyryl forms ligands **d**, **e**, **f**, and **g**, respectively, and allows us to ascertain the effect of different transmitters in ligands on one- and two-photon absorption properties of metal complexes. (2) To study the effect of the nature of metallic centers in metal complexes on one- and two-photon absorption properties of metal complexes. Therefore, we use metal ions Zn(II), Fe(II), and Cu(I) to coordinate with ligands **e**−**g**, respectively, building up dipolar complexes **1a-Zn** to **1g-Zn**, **1c-Fe** and **1c*-Cu**, octupolar tetrahedral complexes **2a*-Zn** to **2g*-Zn** and **2c*-Cu** as well as octahedral complexes **3a-Zn** and **3c-Zn** to **3g-Zn**. Experimentally, the 6,6′-positions of bipyridyl ligands in tetrahedral complexes are often methylated to stabilize the tetrahedral geometry and protect the central metal ion against oxidation, so in this paper, the methyl groups are introduced into the 6,6′-positions of bipyridyl ligands in tetrahedral **2a*-Zn** to **2g*-Zn** and **2c*-Cu** as well as **1c*-Cu**. Finally, by comparing one and two-photon absorption of dipolar, octupolar tetrahedral and octahedral complexes, we can take insight into the effect of symmetry of molecules on one- and two-photon absorption properties of metal complexes.

All the molecular equilibrium geometries have been calculated with the hybrid B3LYP functional combined with the 6-31G basis set using the Gaussian 03 program suite.[34b] The ligands, dipolar complexes, and octupolar tetrahedral and octahedral metal complexes are restricted to C_{2h}, C_{2v}, D_{2d}, and D_3 symmetries, respectively. The calculated results show that the values of the lengths of the N−M (M denotes metal ion) bond and the bond angles N−M−N in the complexes are slightly affected by the nature of the ligands, but greatly by the nature of the metal ions and the molecular geometries. For instance, the N−Zn bond lengths in **1c-Zn**, **1e-Zn**, and **1g-Zn** are 2.059, 2.064, and 2.062 Å, respectively, which are longer than that in **2c*-Zn** (2.007 Å), **2e*-Zn** (2.009 Å), and **2g*-Zn** (2.007 Å). This can be caused by the large electronegativity of chlorine coordinated with Zn(II). The N−Fe bond length in **1c-Fe** and the N−Cu bond lengths in **1c*-Cu** and **2c*-Cu** are 1.866, 1.954, and 1.997 Å, respectively, which are shorter than the N−Zn bond lengths in **1c-Zn** and **2c*-Zn**. We know the ionic radii [0.96 Å for Cu(I) > 0.74 Å for Fe(II) = 0.74 Å for Zn(II)]; therefore, the decrease of the N−M bond lengths on proceeding from **1c-Zn** to **1c-Fe** or **1c*-Cu** as well as from **2c*-Zn** to **2c*-Cu** is not caused by the different sizes of metal ions. The reason is possibly the larger overlaps between the 3d orbitals of the metal ions (Fe(II) and Cu(I)) and the π orbitals of the ligands in Fe(II) and Cu(I) bipyridyl complexes than that in Zn(II) bipyridyl complexes. As the number of ligands increases, the N−Zn bond lengths in octahedral Zn(II) complexes increase

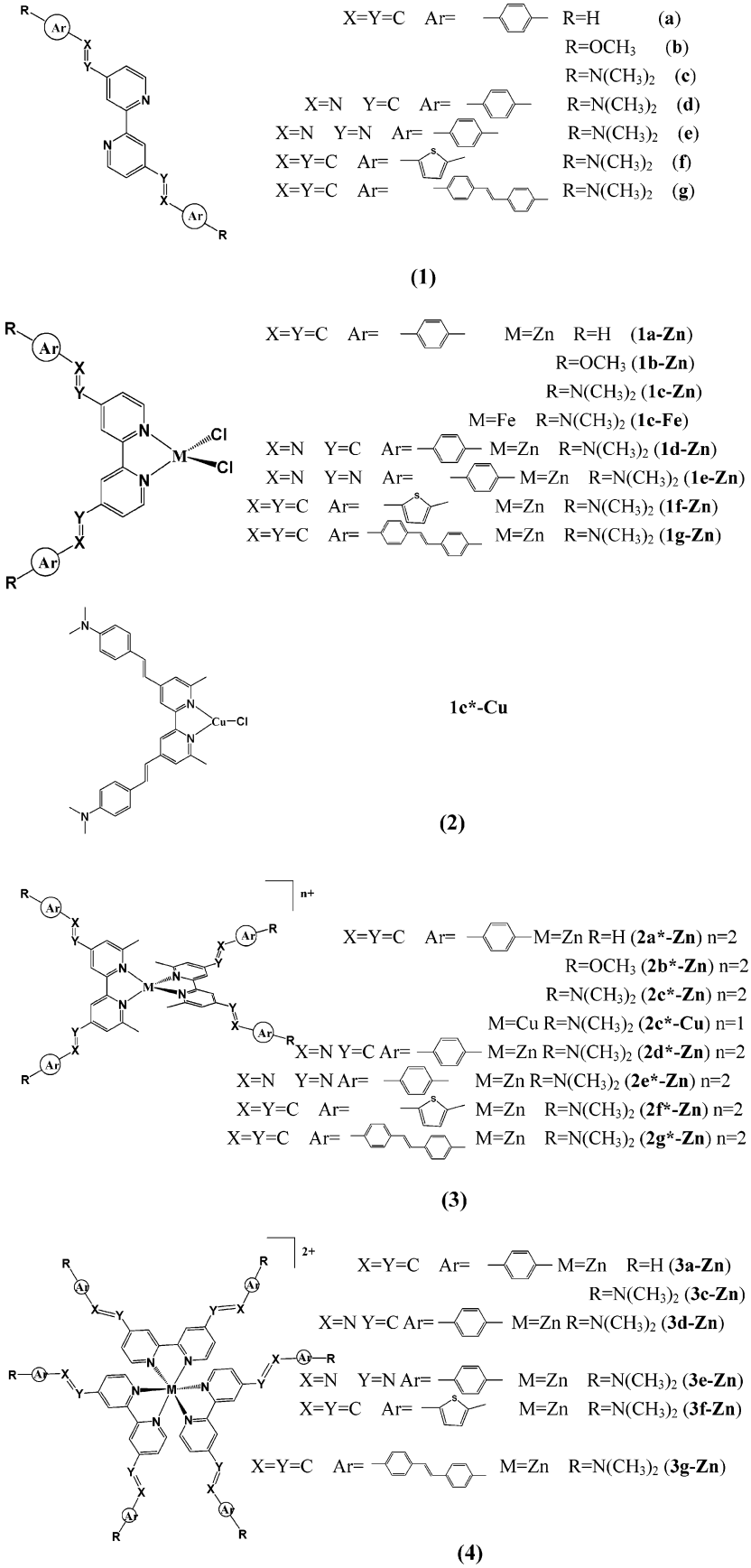

Figure 1. Molecular structures of studied compounds: ligands (1); dipolar metal complexes (2); octupolar tetrahedral complexes (3); octupolar octahedral complexes (4).

relative to that in tetrahedral Zn(II) complexes, due to the increased steric hindrances between ligands. For example, the N−Zn bond lengths in **2c*-Zn** and **3c-Zn** are 2.007 and 2.184 Å, respectively. Under the influence of geometric structures of molecules, the values of the smallest N−Zn−N bond angles in dipolar, octupolar tetrahedral, and octahedral Zn(II) complexes

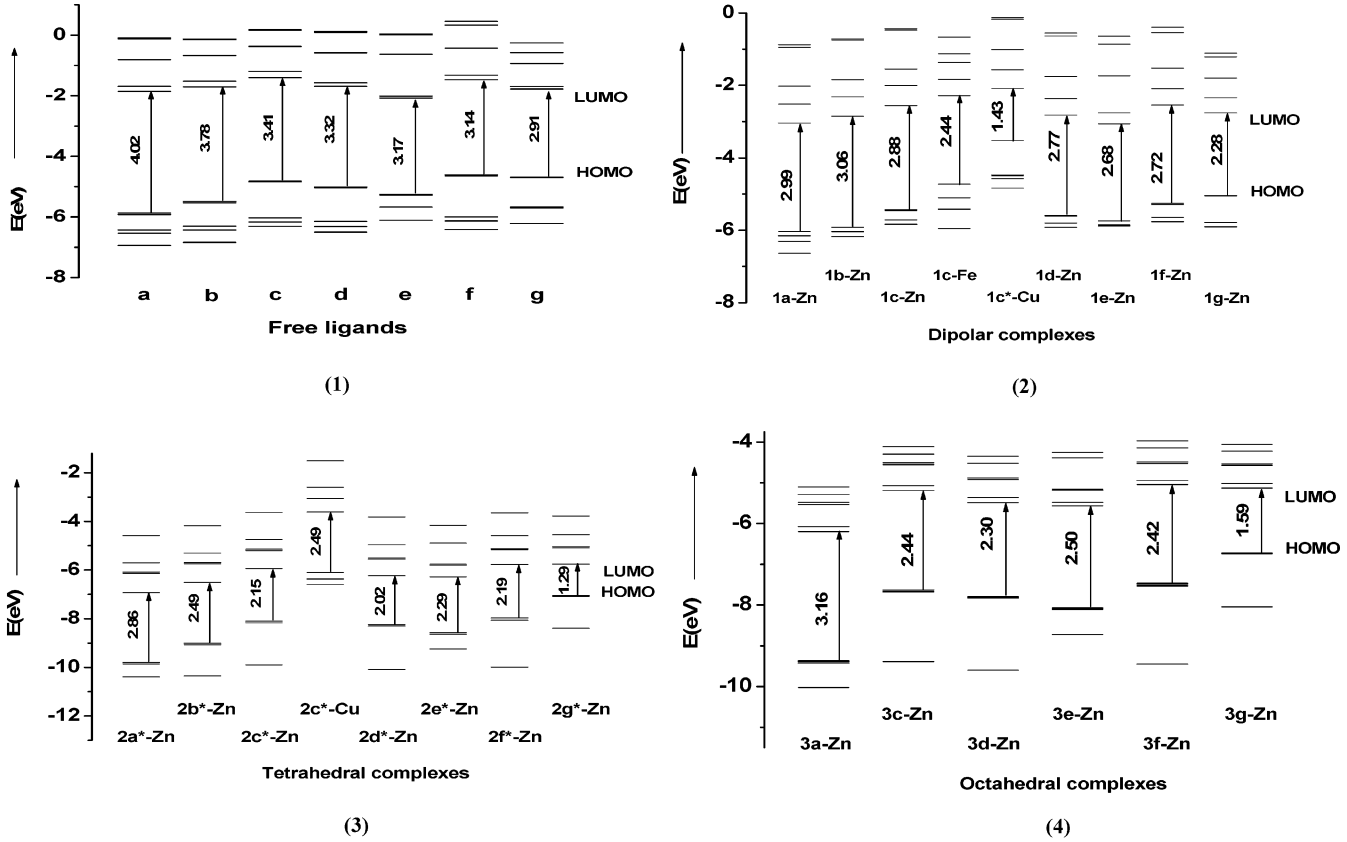

Figure 2. B3LYP/6-31G predicted molecular orbital energy diagram for ligands (1), dipolar metal complexes (2), octupolar tetrahedral metal complexes (3), and octupolar octahedral metal complexes (4).

are about 80.3°, 84.2°, and 75.6°, respectively. The bond angles N−M−N are about 84.2° in complexes **1c-Fe** and **1c*-Cu** and 82.9° in **2c*-Cu**.

Electronic Structures. The calculated energies of the frontier orbitals at the B3LYP/6-31g level are collected in Figure 2. For a given geometric structure (ligand, dipolar zinc(II) complex, octupolar tetrahedral, or octahedral zinc(II) complexes) and a transmitter (styryl ligand), as the strength of the donors increases on going from −H to $-OCH_3$ to $-N(CH_3)_2$, the energies of the HOMO (the highest occupied molecular orbital) and LUMO (the lowest unoccupied molecular orbital) increase and the energy gap between the HOMO and LUMO decreases: such as the HOMO−LUMO energy gap **a** (4.02 eV) > **b** (3.78 eV) > **c** (3.41 eV) and **2a*-Zn** (2.86 eV) > **2b*-Zn** (2.49 eV) > **2c*-Zn** (2.15 eV). However, the influence of the strength of the donors on the HOMO−LUMO energy gap of tetrahedral complexes is smaller, the change tendency of the HOMO−LUMO energy gaps of dipolar complexes is different from those of ligands and octupolar tetrahedral complexes, that is, **1b-Zn** (3.06 eV) > **1a-Zn** (2.99 eV) > **1c-Zn** (2.88 eV). For a given donor $-N(CH_3)_2$, changing the ligands by replacing styryl with bistyryl causes a decrease of the HOMO−LUMO energy gaps in molecules. For instance, 2.15 eV for **2c*-Zn** > 1.29 eV for **2g*-Zn** and 2.44 eV for **3c-Zn** > 1.59 eV for **3g-Zn**. Replacing C═C by C═N and N═N increases the energies of the HOMO and LUMO in **c**, **1c-Zn**, **2c*-Zn**, and **3c-Zn** and makes the HOMO−LUMO energy gaps gradual decrease on going from **c** (3.41 eV) to **d** (3.32 eV) to **e** (3.17 eV) as well as from **1c-Zn** (2.88 eV) to **1d-Zn** (2.77 eV) to **1e-Zn** (2.68 eV), but replacement of C═C with N═N makes the HOMO−LUMO energy gaps of **2e*-Zn** (2.99 eV) and **3e-Zn** (2.50 eV) larger than that of **2c*-Zn** (2.15 eV) and **3c-Zn** (2.44 eV), respectively. The components of molecular orbitals show that in **c**, **1c-Zn**, **2c*-Zn**, and **3c-Zn**, the HOMO is mainly positioned on the *p*-(dimethylamino)styryl moiety, and the LUMO is largely distributed on the bipyridyl moiety. Replacing C═C by C═N and N═N increases the contribution of the *p*-(dimethylamino)-phenyl in the HOMO and decreases the contribution of bipyridyl in the LUMO; at the same time, it increases the contribution of the *p*-(dimethylamino)phenyl to the LUMO (especially in tetrahedral **2e*-Zn** and **3e-Zn**). In the N═N substituted **e**, **2e*-Zn**, and **3e-Zn**, N═N also has an important contribution to the LUMO. The contour surface of the LUMO in **1e-Zn**, which is different from that in other complexes, is mainly distributed on two chlorine atoms (see Figure 1 in the Supporting Information (SI)). It can be found from the above discussion that the contributions of the *p*-(dimethylamino)phenyl greatly lower the energy levels of the HOMOs in **2e*-Zn** and **3e-Zn**, so the HOMO−LUMO energy gaps of **2e*-Zn** and **3e-Zn** are increased relative to **2c*-Zn** and **3c-Zn**, respectively. Due to replacing styryl by thienylvinyl, the energies of the HOMO and LUMO in molecules decrease, for example, **2c*-Zn** > **2f*-Zn** and **3c-Zn** > **3f-Zn**, and the HOMO−LUMO energy gaps also decrease, as **c** (3.41 eV) > **f** (3.14 eV), **1c-Zn** (2.88 eV) > **1f-Zn** (2.72 eV), and **3c-Zn** (2.44 eV) > **3f-Zn** (2.42 eV). But there is an exception that the HOMO−LUMO energy gap of **2c*-Zn** (2.15 eV) is smaller than that of **2f*-Zn** (2.19 eV). Replacing the metal ion Zn(II) in **1c-Zn** and **2c*-Zn** by Fe(II) and Cu(I) makes the energy levels of the HOMO and LUMO in **1c-Fe**, **1c*-Cu**, and **2c*-Cu** higher than those in **1c-Zn** and **2c*-Zn**, respectively, due to the different natures of metal ions. Comparing the energy level diagrams of ligands, dipolar complexes, and octupolar tetrahedral and octahedral complexes, we can find that complexation of ligands with metal ions decreases the HOMO−LUMO energy gaps of ligands; the

TABLE 1: OPA Properties for Studied Compounds

molecule	transition nature	λ^{O}_{max}/nm	oscillator strength (*f*)	molecule	transition nature	λ^{O}_{max}/nm	oscillator strength (*f*)
a	$S_0 \rightarrow S_1$	379.4	0.605	**1g-Zn**	$S_0 \rightarrow S_1$	463.0	1.893
	$S_0 \rightarrow S_5$	345.8	1.555		$S_0 \rightarrow S_2$	437.7	1.587
b	$S_0 \rightarrow S_1$	386.2	0.952	**2a*-Zn**	$S_0 \rightarrow S_{1(2)}$	495.9	1.001
	$S_0 \rightarrow S_5$	359.3	1.265		$S_0 \rightarrow S_3$	474.3	2.002
c	$S_0 \rightarrow S_1$	395.4 (397)[29]	1.513	**2b*-Zn**	$S_0 \rightarrow S_{1(2)}$	536.7	1.024
	$S_0 \rightarrow S_4$	369.7	0.803		$S_0 \rightarrow S_3$	511.0	2.162
d	$S_0 \rightarrow S_1$	409.5 (433)[26]	1.692	**2c*-Zn**	$S_0 \rightarrow S_{1(2)}$	569.0	1.039
					$S_0 \rightarrow S_3$	541.2 (529)[27]	2.302
e	$S_0 \rightarrow S_3$	458.7 (471)[26]	1.713	**2c*-Cu**	$S_0 \rightarrow S_1$	467.1 (484)[25]	1.846
					$S_0 \rightarrow S_{4(5)}$	452.0 (424)[25]	1.172
f	$S_0 \rightarrow S_1$	428.9	1.922	**2d*-Zn**	$S_0 \rightarrow S_{1(2)}$	636.1	1.020
					$S_0 \rightarrow S_3$	613.3	1.548
g	$S_0 \rightarrow S_1$	426.1	3.608	**2e*-Zn**	$S_0 \rightarrow S_{1(2)}$	567.0	1.228
					$S_0 \rightarrow S_3$	538.5	2.521
1a-Zn	$S_0 \rightarrow S_1$	403.7	1.113	**2f*-Zn**	$S_0 \rightarrow S_{1(2)}$	649.2	1.141
	$S_0 \rightarrow S_2$	374.5	0.782		$S_0 \rightarrow S_3$	608.7	2.375
1b-Zn	$S_0 \rightarrow S_1$	423.4	1.159	**2g*-Zn**	$S_0 \rightarrow S_{1(2)}$	632.6	1.141
	$S_0 \rightarrow S_2$	395.1	0.872		$S_0 \rightarrow S_3$	606.7	2.317
1c-Zn	$S_0 \rightarrow S_1$	444.5 (459)[26]	1.160	**3a-Zn**	$S_0 \rightarrow S_3$	428.2	1.818
	$S_0 \rightarrow S_2$	415.3	0.956		$S_0 \rightarrow S_{4(5)}$	413.9	1.538
1c-Fe	$S_0 \rightarrow S_4$	548.1	0.032	**3c-Zn**	$S_0 \rightarrow S_3$	474.6	1.448
	$S_0 \rightarrow S_6$	449.6	1.225		$S_0 \rightarrow S_{4(5)}$	462.7 (466)[27]	1.914
	$S_0 \rightarrow S_7$	443.2	0.422				
1c*-Cu	$S_0 \rightarrow S_2$	425.0	1.261	**3d-Zn**	$S_0 \rightarrow S_3$	531.4	1.373
	$S_0 \rightarrow S_4$	397.1	0.970		$S_0 \rightarrow S_{4(5)}$	521.8	1.281
1d-Zn	$S_0 \rightarrow S_1$	468.6 (491)[26]	1.004	**3e-Zn**	$S_0 \rightarrow S_3$	504.0	2.132
	$S_0 \rightarrow S_2$	447.0	0.623		$S_0 \rightarrow S_{4(5)}$	484.2	1.962
1e-Zn	$S_0 \rightarrow S_1$	502.3 (516)[26]	1.025	**3f-Zn**	$S_0 \rightarrow S_3$	562.1	1.947
	$S_0 \rightarrow S_2$	470.2	0.831		$S_0 \rightarrow S_{4(5)}$	539.0	2.039
1f-Zn	$S_0 \rightarrow S_1$	500.4	1.125	**3g-Zn**	$S_0 \rightarrow S_3$	516.4	1.687
	$S_0 \rightarrow S_2$	465.3	0.888		$S_0 \rightarrow S_{4(5)}$	508.4	1.930

HOMO−LUMO energy gaps of octahedral complexes are larger than that of tetrahedral complexes.

One-Photon Absorption. Table 1 summarizes the calculated one-photon absorption (OPA) properties (the maximum OPA wavelengths λ^{O}_{max}, transition natures, and oscillator strengths *f*) of studied molecules and the available experimental values. As shown in Table 1, our calculated results are in agreement with the experimental values. The maximum OPA wavelengths of ligands are successively red-shifted with the increased donor strength from **a** (345.8 nm) to **b** (359.3 nm) to **c** (395.4 nm). On proceeding from **c** to **g**, due to the increased chain length, the maximum OPA wavelength is red-shifted by 30.7 nm from 395.4 to 426.1 nm. Replacing the C═C in **c** by C═N and N═N causes the maximum one-photon absorptions to be red-shifted. The maximum OPA wavelength of **c** is 395.4 nm, and the maximum OPAs of the C═N and N═N substituted **d** and **e** occur at 409.5 and 458.7 nm, respectively. The maximum OPA is red-shifted by 33.5 nm from 395.4 nm for **c** to 428.9 nm for **f**, due to replacing styryl by thienylvinyl. Replacing a benzene ring with a thiophene ring reduces the resisting aromatic delocalization (aromatic stabilization energies: 29 kcal/mol for a thiophene ring and 36 kcal/mol for a benzene ring, respectively) in the highly aromatic benzene ring and hence leads to an increase in the electron transmission between the donor ($-N(CH_3)_2$) and acceptor (bipyridyl), decreasing the energy gap between the ground state and the OPA state and increasing the corresponding transition moment. In addition, the electron-rich thienyl ring weakly withdraws excessive electron density from the donor substituent $-N(CH_3)_2$ through inductive effect, thereby increasing the donor ability of the donor $-N(CH_3)_2$. Upon coordination, the acceptor strength of the pyridinic ring is enhanced, resulting in a red shift of the maximum OPA wavelength. For example, for a given ligand such as **c**, a red shift of 49.1 nm from 395.4 nm for **c** to 444.5 nm for **1c-Zn** is obtained. The maximum OPAs of metal complexes are strongly influenced by the symmetry of molecules. λ^{O}_{max} (octupolar tetrahedral complexes) > λ^{O}_{max} (octupolar octahedral complexes) > λ^{O}_{max} (dipolar complexes). The maximum OPA wavelengths of **2c*-Zn** and **3c-Zn** are 569.0 and 531.4 nm, respectively, which are red-shifted by 124.5 and 30.1 nm, respectively, relative to that of **1c-Zn** (444.5 nm). Apparently, octahedral complexes are more promising candidates for TPA materials than tetrahedral complexes from the transparency point of view. In metal complexes, when changing the styryl linkage to a distyryl or thienylvinyl linkage, the maximum OPA is steadily red-shifted. For instance, **2c*-Zn** (444.5 nm) < **2g*-Zn** (463.0 nm) < **2f*-Zn** (500.4 nm) as well as **3c-Zn** (474.6 nm) < **3g-Zn** (516.4 nm) < **3f-Zn** (562.1 nm). Due to replacing C═C by C═N and N═N, the maximum OPAs are gradually red-shifted on going from **1c-Zn** (444.5 nm) to **1d-Zn** (468.6 nm) to **1e-Zn** (502.3 nm), as found with the corresponding bipyridyl ligands. But replacing the C═N in **2d*-Zn** and **3d-Zn** by N═N leads to the blue shifts of 69.1 and 27.4 nm (636.1 nm for **2d*-Zn** vs 567.0 nm for **2e*-Zn** and 531.4 nm for **3d-Zn** vs 504.0 nm for **3e-Zn**), respectively. The influence of the central metallic ion on the one-photon absorptions of metal complexes is examined by using the same bipyridyl ligand **c**. As the Lewis acidity changes in the order Cu(I) < Fe(II) ≈ Zn(II), the maximum OPA is red-shifted by 24.6 nm from **1c*-Cu** (425.0 nm) to 1**c-Fe** (449.6 nm) and by 101.9 nm from **2c*-Cu** (467.1 nm) to **2c*-Zn** (569 nm), and **1c-Zn** and **1c-Fe** have roughly similar maximum OPA wavelengths (444.5 nm vs 449.6 nm). Table 2 collects the ZINDO calculated net charges of metal ions in the ground (Q_0) and the maximum OPA states (Q) and the difference of them (ΔQ). As shown in Table 2, the net charges on M in both the ground and the maximum OPA states of dipolar and octupolar tetrahedral Zn(II) complexes as

TABLE 2: ZINDO Calculated Net Charges of Metal Ions in the Ground (Q_0) and the Maximum OPA States (Q) and the Difference of Them (ΔQ)

moleucle	Q_0	Q_n	ΔQ	molecule	Q_0	Q_n	ΔQ
1a-Zn	0.127	0.127	0.000	**2c*-Cu**	−0.268	−0.052	0.216
1b-Zn	0.126	0.126	0.000	**2d*-Zn**	0.058	0.057	−0.001
1c-Zn	0.125	0.125	0.000	**2e*-Zn**	0.053	0.053	0.000
1c-Fe	0.296	0.352	0.056	**2f*-Zn**	0.049	0.049	0.000
1c*-Cu	−0.051	−0.037	0.014	**2g*-Zn**	0.052	0.051	−0.001
1d-Zn	0.128	0.128	0.00	**3a-Zn**	−0.014	−0.014	0.000
1e-Zn	0.126	0.126	0.00	**3c-Zn**	−0.017	−0.017	0.000
1f-Zn	0.125	0.125	0.00	**3d-Zn**	−0.012	−0.013	−0.001
1g-Zn	0.126	0.126	0.00	**3e-Zn**	−0.015	−0.015	0.000
2a*-Zn	0.056	0.056	0.00	**3f-Zn**	−0.018	−0.018	0.000
2b*-Zn	0.054	0.054	0.00	**3g-Zn**	−0.017	−0.017	0.000
2c*-Zn	0.052	0.052	0.00				

well as **1c-Fe** are positive values, whereas in octahedral Zn(II) complexes and **1c*-Cu** and **2c*-Cu**, the values of the net charges are negative. From the values of ΔQ, it can be found that during one-photon excitation, the net charge change on M in the Fe(II) and Cu(I) complexes is large and its sign is positive (0.056 for **1c-Fe**, 0.014 for **1c*-Cu**, and 0.216 for **2c*-Cu**), whereas the values of the net charges on Zn in Zn(II) complexes are very small, indicating that the metal ions in Cu(I) and Fe(II) complexes participate in the one-photon excitation and the charge transfers are from the metal ions to ligands whereas the Zn(II) in Zn(II) complexes nearly do not take part in this process. This is related to high third-ionization potential of zinc.

Two-Photon Absorption. The two-photon absorption (TPA) properties of studied molecules are calculated by using the ZINDO-SOS method, which is extensively employed to calculation on TPA properties of many systems and proved to be reliable.[5,20c,35] The calculated results (the positive TPA cross section values and the corresponding TPA wavelength) are collected in Figure 3, and the calculated maximum TPA wavelengths λ_{max}^{T}, the maximum TPA cross sections δ_{max}, the transition natures, and the imaginary parts of the relevant third-order susceptibilities are tabulated in Table 3. To further examine our method, the TPA property of zinc(II) meso,meso-coupled porphyrin dimer (**Z2$_H$-G**) via intermolecular hydrogen bonding interactions, the TPA cross section of which is available in the literature,[36] was calculated. As shown in Table 3, our calculated results are in good agreement with the experimental values. It can be found from Figure 3 that ligands **a**−**c** exhibit the maximum TPA (1767−2141 GM) in the range 550−590 nm, with a weak peak (158−495 GM) in the range 675−740 nm. As the donor strength increases, the TPA peak values increase, and the TPA peak positions are slightly red-shifted on going from **a** to **c**. Replacing the styryl linkage in **c** with a phenylimino, phenylazo, thienylvinyl, or bistyryl linkage forms **d**−**g**. The maximum TPA wavelengths of **d**, **e**, and **g** (584.2 nm vs 592.4 nm vs 600.6 nm) are approximately same as that of **c** (589.8 nm). The maximum TPA wavelength of **f** is 655.4 nm, which is red-shifted by 65.6 nm relative to that of **c**. Molecules **d** and **c** have nearly the same maximum TPA cross sections (2164.6 GM vs 2140.8 GM, respectively). The maximum TPA cross sections of **e** and **g** are 7173.6 and 20854.7 GM, respectively, which are 9.7 and 3.4 times that of **c** (2140.8 GM), respectively. The maximum TPA cross section of the thienylvinyl substituted **f** (1605.1GM) is decreased by 535.7 GM relative to **c** (2140.8 GM), which is different from the quadratic nonlinear optical properties. Replacing styryl with thienylvinyl leads to a 10% enhancement of molecular hyperpolarizability.[28] Due to replacing C═C with C═N and N═N, the second TPA peak positions of **d** (786.4 nm) and **e** (871.6 nm) are red-shifted by 50.2 and 135.4 nm, respectively, relative to **c** (736.2 nm). Complexation with metal ions greatly increases the TPA cross sections of ligands, because complexation with metal ions increases the electron-accepting ability of bipyridyl. The maximum TPA cross sections of the dipolar **1a-Zn**, **1b-Zn**, **1c-Zn**, and **1d-Zn** are 7011.2, 7631.6, 1000.3, and 14889.9 GM, respectively, which are 4.0, 3.6, 4.7, and 6.9 times that of the corresponding ligands **a**, **b**, **c**, and **d**, respectively. The maximum TPA cross sections of **1e-Zn** to **1g-Zn** are increased to be 5238.1, 1722.8, and 2721.5 GM, respectively, relative to ligands **e**−**g**. Due to complexation with metal ions, the second TPA peaks of **a**−**g** are red-shifted and the corresponding peak values are increased. For example, the second absorption peak value for **1g-Zn** is 1628.4 GM, which is 3.9 times that of **g** (416.7 GM). In the range 500−1250 nm, octupolar tetrahedral and octahedral complexes exhibit intense TPAs. On proceeding from dipolar Zn(II) complexes to octupolar tetrahedral Zn(II) complexes, due to the influence of geometry of molecules, the maximum TPA wavelengths are greatly red-shifted (>350 nm). For instance, the maximum TPAs of **2d*-Zn** and **2g*-Zn** are red-shifted by 553.2 and 507.6 nm relative to **1d-Zn** and **1g-Zn**, respectively. The maximum TPA cross sections of **2a*-Zn** to **2g*-Zn** are in the range 3081−29215 GM. Due to decrease in conjugated effects caused by increased hindrances among ligands, the maximum TPA wavelengths are blue-shifted from octupolar tetrahedral to octahedral complexes. For example, the maximum TPA wavelength is blue-shifted by 159.2 nm from 1095 nm for **2d*-Zn** to 935.8 for **3d-Zn** nm. As the number of ligands increases, the maximum TPA cross section increases on going from octupolar tetrahedral to octahedral complexes. The maximum TPA cross sections of octahedral complexes are in the range 5607−25098 GM. For instance, the maximum TPA cross section of **3d-Zn** is 13385.4 GM, which is increased by 3133 GM relative to **2d*-Zn** (10252.4 GM). The TPA peak value of **3g-Zn** (at long wavelength) is increased by 1644.2 GM relative to that of **2g*-Zn**. Comparing the influence of the nature of ligands on the TPA properties of metal complexes, one can see that the maximum TPA cross section increases with the strength of donors, accompanied by the red shift of the TPA wavelength. Due to replacement of −H by $-N(CH_3)_2$, the maximum TPA wavelength of **3c-Zn** is red-shifted by 219.4 nm relative to **3a-Zn** (969.2 nm for **3c-Zn** vs 749.8 nm for **3a-Zn**, respectively), and the corresponding TPA cross section is increased by 4325.7 GM. In dipolar metal complexes, replacing the C═C in **1c-Zn** by C═N and N═N increases the maximum TPA responses on going from **1d-Zn** (14889.9 GM) to **1e-Zn** (12411.7 GM) to **1c-Zn** (10000.3 GM). Tetrahedral complexes **2c*-Zn** and **2e*-Zn** have nearly the same maximum TPA cross sections (6287.8 GM for **2c*-Zn** and 6419.3 GM for **2e*-Zn**, respectively). In octahedral complexes, the maximum TPA cross section of **3c-Zn** is larger than that of **3e-Zn**

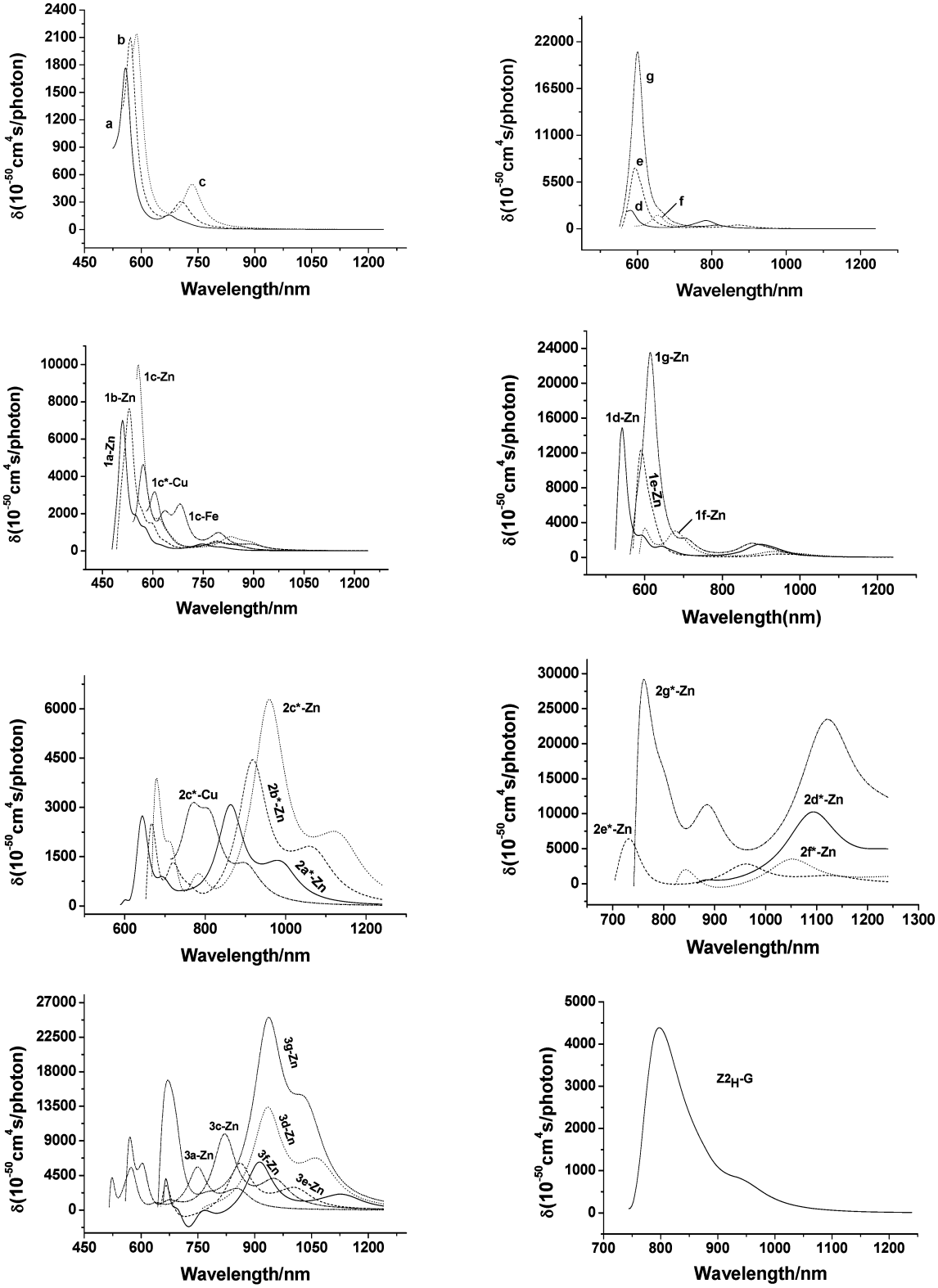

Figure 3. TPA spectra for studied compounds.

(9932.9 GM vs 6097.1 GM, respectively). The ZINDO calculated results show that among the C═C, C═N, and N═N substituted complexes, the C═N substituted complexes all exhibited the largest TPA cross section. Replacing styryl with thienylvinyl leads to decrease of the maximum TPA cross sections. The maximum TPA cross sections of **1f-Zn**, **2f*-Zn**, and **3f-Zn** are decreased by 6672.4, 2759.4, and 3693.9 GM relative to **1c-Zn**, **2c*-Zn**, and **3c-Zn**, respectively. Although replacing styryl with thienylvinyl increases the electronic couplings between the ground and lowest lying excited states through the transition dipole moment, at the same time, it decreases the couplings between the excited states. For example, the transition dipole moment between the ground state and the fourth or fifth excited state in **3c-Zn** (12.1 or 13.7 Debye) is smaller than that in **3f-Zn** (15.2 or 15.3 Debye), but the transition dipole moment between the third and sixth state (9.0 Debye) in **3c-Zn** is larger than that in **3f-Zn** (5.8 Debye) (see Figure 2 in the SI). Therefore, the decrease of the transition

TABLE 3: TPA Properties for Studied Compounds

molecule	transition nature	λ^{T}_{max}/nm	Im $\gamma/10^{-34}$ esu	δ_{max}/GM	molecule	transition nature	λ^{T}_{max}/nm	I$m\gamma/10^{-34}$ esu	δ_{max}/GM
a	$S_0 \rightarrow S_6$	675.0	10.4	158.3	**2a*-Zn**	$S_0 \rightarrow S_4$	864.2	331.6	3081.9
	$S_0 \rightarrow S_{10}$	559.4	79.9	1767.4		$S_0 \rightarrow S_{15}$	644.4	164.7	2740.8
b	$S_0 \rightarrow S_6$	705.8	22.2	307.1	**2b*-Zn**	$S_0 \rightarrow S_4$	919.6	545.1	4452.2
	$S_0 \rightarrow S_{10}$	572.0	99.3	2102.2		$S_0 \rightarrow S_{13(14)}$	719.2	99.5	1323.7
						$S_0 \rightarrow S_{19}$	664.8	162.3	2517.8
c	$S_0 \rightarrow S_5$	736.2	38.5	493.6	**2c*-Zn**	$S_0 \rightarrow S_4$	961.0	835.5	6287.8
	$S_0 \rightarrow S_{10}$	589.8	106.9	2140.8		$S_0 \rightarrow S_7$	780.8	87.5	984.4
						$S_0 \rightarrow S_{19}$	674.4	258.5	3882.1
d	$S_0 \rightarrow S_2$	786.4	86.0	967.4	**2c*-Cu**	$S_0 \rightarrow S_8$	765.8	271.9	3151.5
	$S_0 \rightarrow S_{12}$	584.2	105.8	2164.6					
e	$S_0 \rightarrow S_4$	871.6	48.9	447.2	**2d*-Zn**	$S_0 \rightarrow S_4$	1095.0	1780.1	10252.4
	$S_0 \rightarrow S_{15}$	592.4	366.8	7173.6					
f	$S_0 \rightarrow S_2$	813.4	42.4	444.7	**2e*-Zn**	$S_0 \rightarrow S_4$	962.2	379.6	2830.6
	$S_0 \rightarrow S_6$	655.4	99.6	1605.1		$S_0 \rightarrow S_{12}$	736.8	485.8	6419.3
g	$S_0 \rightarrow S_2$	815.8	39.7	416.7	**2f*-Zn**	$S_0 \rightarrow S_4$	1053.8	563.8	3528.4
	$S_0 \rightarrow S_{12}$	600.6	1084.9	20854.7		$S_0 \rightarrow S_{5(6)}$	847.4	206.4	2015.6
1a-Zn	$S_0 \rightarrow S_2$	749.0	30.0	372.0	**2g*-Zn**	$S_0 \rightarrow S_4$	1122.6	4250.5	23453.6
	$S_0 \rightarrow S_{20}$	508.6	263.3	7011.2		$S_0 \rightarrow S_8$	885.8	1277.8	11289.0
						$S_0 \rightarrow S_{16}$	758.6	2446.5	29214.8
1b-Zn	$S_0 \rightarrow S_2$	790.2	48.1	533.2	**3a-Zn**	$S_0 \rightarrow S_3$	856.4	296.8	2828.3
	$S_0 \rightarrow S_{13}$	533.2	310.6	7631.6		$S_0 \rightarrow S_6$	749.8	456.0	5607.2
						$S_0 \rightarrow S_{36}$	575.2	264.7	5540.3
						$S_0 \rightarrow S_{57}$	523.8	167.8	4229.0
1c-Zn	$S_0 \rightarrow S_2$	830.6	77.0	770.3	**3c-Zn**	$S_0 \rightarrow S_3$	949.2	539.0	4132.1
	$S_0 \rightarrow S_{12}$	556.6	447.4	10000.3		$S_0 \rightarrow S_6$	822.0	969.2	9932.9
						$S_0 \rightarrow S_{36}$	603.4	320.5	6088.5
1c-Fe	$S_0 \rightarrow S_9$	797.6	90.8	991.0	**3d-Zn**	$S_0 \rightarrow S_3$	1062.8	1104.9	6774.8
	$S_0 \rightarrow S_{22}$	571.6	219.0	4634.9		$S_0 \rightarrow S_6$	935.8	1698.9	13385.4
1c*-Cu	$S_0 \rightarrow S_4$	794.2	42.4	466.3	**3e-Zn**	$S_0 \rightarrow S_3$	1008.0	430.3	2944.7
	$S_0 \rightarrow S_{15}$	604.0	168.5	3182.0		$S_0 \rightarrow S_6$	862.2	656.0	6097.1
						$S_0 \rightarrow S_{18}$	665.0	203.1	3172.0
1d-Zn	$S_0 \rightarrow S_2$	894.0	175.5	1511.2	**3f-Zn**	$S_0 \rightarrow S_3$	1124.2	377.2	2058.6
	$S_0 \rightarrow S_{20}$	541.8	631.7	14889.9		$S_0 \rightarrow S_6$	914.0	750.5	6239.0
						$S_0 \rightarrow S_{28(29)}$	666.0	260.5	4068.0
1e-Zn	$S_0 \rightarrow S_2$	940.4	49.6	383.6	**3g-Zn**	$S_0 \rightarrow S_6$	937.2	3185.5	25097.8
	$S_0 \rightarrow S_{12}$	593.6	627.4	12411.7		$S_0 \rightarrow S_{36}$	671.6	1102.8	16890.4
1f-Zn	$S_0 \rightarrow S_2$	930.6	85.5	680.0	**Z2$_H$-G**	$S_0 \rightarrow S_{15}$	802.6 (800)[36,37]	405.3	4387.5 (4500)[36,37]
	$S_0 \rightarrow S_6$	674.6	201.5	3026.2					
	$S_0 \rightarrow S_{10}$	596.0	173.1	3327.9					
1g-Zn	$S_0 \rightarrow S_2$	875.4	181.2	1628.4					
	$S_0 \rightarrow S_{12}$	615.0	1285.5	23576.2					

dipole moments between the excited states is the main reason for the reduced values of the TPA cross sections on going from the metal complexes with styryl to the metal complexes with thienylvinyl. In studied dipolar, tetrahedral, and octahedral complexes, **1g-Zn**, **2g*-Zn**, and **3g-Zn** have the maximum TPA cross sections (23576.2 GM for **1g-Zn**, 29214.8 GM for **2g*-Zn**, and 25097.8 GM for **3g-Zn**, respectively), indicating that of all the influence factors of ligands, the increase of conjugated chain length of the ligands has the most important effect on the TPA cross section of the complex. The TPA properties of the metal complexes are also strongly correlated with the metal Lewis acidity. Complexes **1c-Zn** and **1c-Fe** have almost the same maximum TPA wavelength (556.6 nm for **1c-Zn** vs 571.6 nm for **1c-Fe**, respectively), due to the similar Lewis acidities of Zn(II) and Fe(II). The maximum TPA cross section of **1c-Fe** is decreased by 5365.4 GM from 10000.3 GM for **1c-Zn** to 4634.9 GM for **1c-Fe**. Due to the Lewis acidity of Cu(I) being less than that of Zn(II), the maximum TPA wavelength of **2c*-Cu** is blue-shifted by 195.2 nm relative to that for **2c*-Zn** (765.8 nm for **2c*-Cu** and 961.0 nm for **2c*-Zn**, respectively). The maximum TPA cross section of **2c*-Zn** is nearly twice that of **2c*-Cu** (6287.8 GM for **2c*-Zn** and 3151.5 GM for **2c*-Cu**).

Generally, the frontier molecular orbitals, especially HOMO−1, HOMO, LUMO, and LUMO+1, have important contributions to the electronic transition during two-photon excitation. Now, we will analyze the influence of the nature of metal ion on the TPA properties of pyridyl metal complexes in terms of the contours of the frontier orbitals. In Figure 4 we plot the contours of the HOMO−1, HOMO, LUMO and LUMO+1 for **1c-Zn**, **1c-Fe**, **2c*-Zn**, and **2c*-Cu**. In the case of **1c-Zn** or **2c*-Zn**, the HOMO−1 and HOMO are mainly distributed on the *p*-(dimethylamino)phenyl moiety, and the LUMO and LUMO+1 are mainly positioned on the bipyridyl moiety. Therefore, the transitions between the HOMO−1, HOMO, LUMO and LUMO+1 in the **1c-Zn** or **2c*-Zn** are only accompanied by the charge transfer from the *p*-(dimethylamino)phenyl moiety to the bipyridyl moiety (i.e., ILCT transitions). In the **1c-Fe**, the HOMO−1 is mainly positioned on the *p*-(dimethylamino)-phenyl moiety, the Fe(II) and two chlorine atoms and the HOMO are mainly positioned on the Fe(II) and two chlorine atoms, whereas the LUMO and LUMO+1 are mainly distributed on the bipyridyl moiety. In **2c*-Cu**, the HOMO−1 is positioned on the central Cu(I) ion and the HOMO is distributed on the Cu(I) and p-(dimethylamino)phenyl moiety; the LUMO and LUMO+1 have important contributions from the bipyridyl moiety. Therefore, during the transitions between the HOMO−1, HOMO, LUMO and LUMO+1 in **1c-Fe** or **1c-Cu**, there are charge transfers from the *p*-(dimethylamino)phenyl moiety to the bipyridyl moiety (ILCT) as well as from the Fe(II) or Cu(I) to the bipyridyl moiety (MLCT). From Figure 4, it can be found that in a first approximation, the ILCT and MLCT in **1c-Fe** and **2c*-Cu** are roughly parallel but in opposite direction. So,

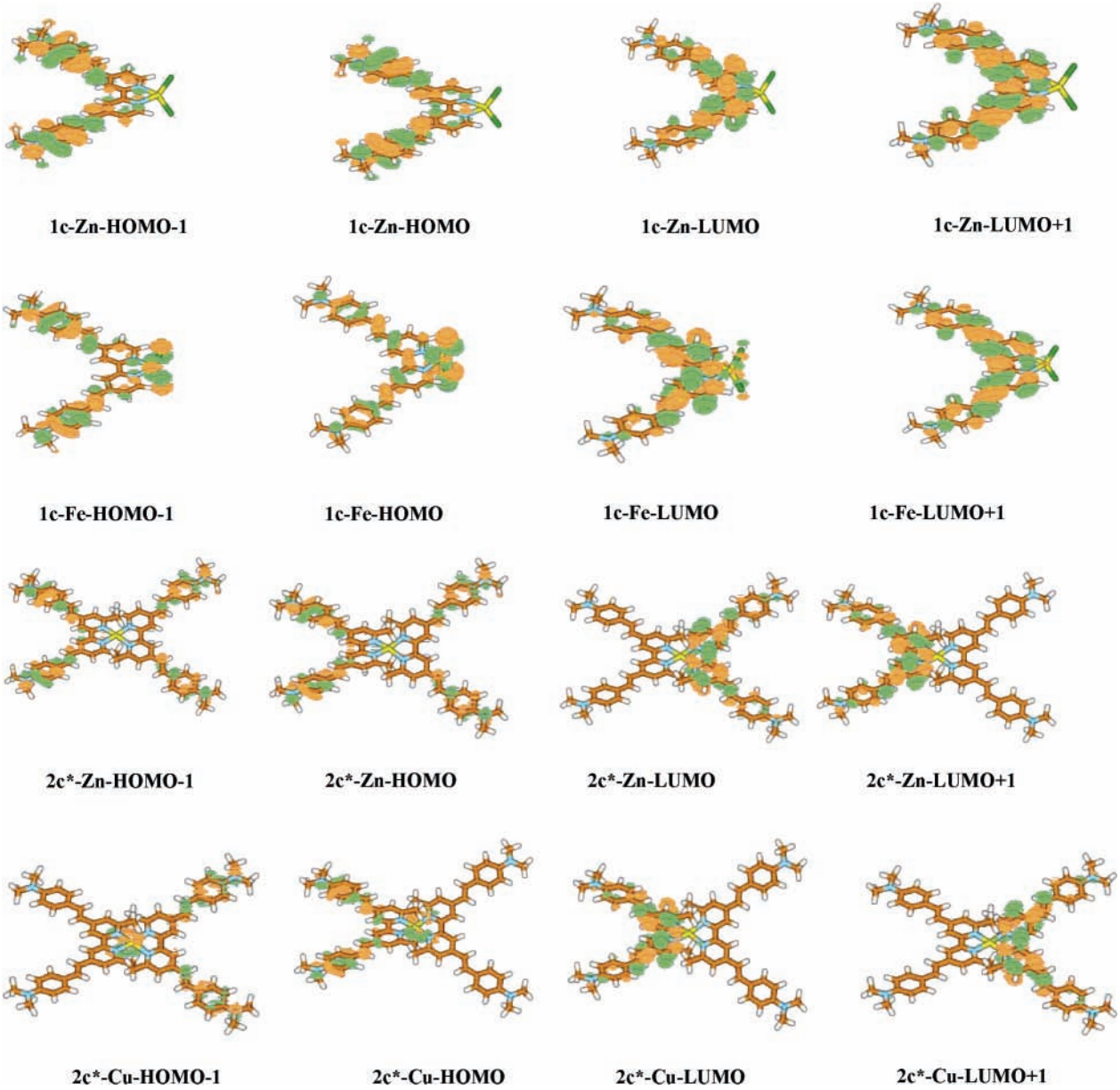

Figure 4. Contour surfaces of HOMO−1, HOMO, LUMO and LUMO+1 for 1c-Zn, 1c-Fe, 2c*-Zn and 2c*-Cu.

in **1c-Fe** and **2c*-Cu**, the contributions from ILCT and MLCT to the TPA cross sections are opposite in sign and counteract each other, whereas in **1c-Zn** and **2c*-Zn**, there only exists ILCT, leading to the TPA cross sections **1c-Zn** > **1c-Fe** and **2c*-Zn** > **2c*-Cu**.

Comparing the one- and two-photon absorption properties of dipolar and octupolar complexes, one can see that the desirable TPA cross sections in the range 500−1250 nm can be obtained by tuning the nature of ligands and metal ions as well as the symmetry of molecules. Especially, on proceeding from dipolar to octupolar octahedral metal complexes, the maximum TPA wavelengths are red-shifted by 240−400 nm, and the corresponding TPA cross sections still remain the large magnitudes, without the undesirable red shift of the one-photon absorptions ($\Delta\lambda = 24-63$ nm). Compared with the TPA cross sections in the long-wavelength region for the dipolar complexes, the TPA cross sections of the octahedral complexes are greatly increased (>3 times). For example, the TPA cross section in 937.2 nm for **3g-Zn** is increased by 15.4 times relative to that in 875.4 nm for **1g-Zn** (25097.8 GM for **3g-Zn** vs 1628.4 GM for **1c-Zn**, respectively). This illustrates the superiority of octupoles versus dipoles in terms of nonlinearity without the significant cost of transparency. Recently, Ikeda and Ahn et al.[36,37] studied the TPA properties of zinc(II) meso−meso linked porphyrin oligomers via intermolecular hydrogen bonding interactions and pointed out that the TPA cross section at 800 nm for $\mathbf{Z2_H}$**-G** (dimer) is 4500 GM, which is consistent with our calculated 4387.5 GM. The TPA cross section of $\mathbf{Z8_H}$**-G** (octamer) is 12800 GM. In our calculated complexes, the **2g*-Zn**, **3d-Zn**, and **3g-Zn** all exhibit the large TPA cross section values (>13000 GM) and the corresponding TPA wavelengths are larger than 900 nm. Therefore, compared with zinc(II) meso−meso linked porphyrin oligomers via intermolecular hydrogen bonding interactions, the zinc(II) complexes with bipyridyl ligands will be better candidates for TPA materials. And the ability to substitute the pyridine rings with functional groups offers the possibility of making macroscopic assemblies featuring octupolar chromophores such as polymers and dendrimers, which is crucial to its application in photonic devices.

Conclusion

In this paper, the molecular equilibrium structures, electronic structures, and one- and two-photon absorption properties of dipolar, octupolar tetrahedral, and octahedral metal complexes have been systematically investigated. Our calculations show that in comparison with dipolar complexes, octupolar complexes exhibit the intense two-photon absorptions in the range 500−1250 nm. And the two-photon absorption properties of complexes are strongly influenced by the nature of ligands and metal ions as well as the symmetry of the complexes. As the strength of the donor groups increases, the maximum TPA wavelengths of complexes are slightly red-shifted and the maximum TPA cross sections are increased. Substitution of the conjugation bridge C═N and N═N for C═C plays an important role in altering the two-photon absorption position and cross section. Of them, the C═N substituted complexes have relatively large TPA cross sections. Replacing styryl with thienylvinyl leads to the red shift of the maximum TPA wavelengths and to the great decrease of the maximum TPA cross sections. The elongation of the π-conjugated backbone is key to maximizing the TPA activity. Complexes **1g-Zn**, **2g*-Zn**, and **3g-Zn** have the largest TPA cross sections in studied dipolar, octupolar tetrahedral, and octahedral complexes, respectively. With regard to the metal ion, the increase of its Lewis acidity results in a significant enhancement of the TPA cross section. In the Fe(II) and Cu(I) complexes, the existence of MLCT nearly antiparallel to ILCT is the main reason for the decrease of the TPA activity relative to that for Zn(II) complexes. On proceeding from octupolar tetrahedral to octahedral complexes, an increased ligand-to-metal ratio causes a blue shift of the maximum TPA wavelengths and a substantial enhancement of the maximum TPA cross sections. The metal complexes in this paper possess a large occurrence of TPA; therefore, the desirable TPA properties can be obtained by tuning the nature of ligands and metal ions as well as the symmetry of the metal complexes. They are promising candidates for TPA materials. At the same time, we expect that our calculated results can provide useful information for experimental scientists in synthesizing new TPA materials.

Acknowledgment. This work is supported by the National Nature Science Foundation of China and the Key Laboratory for Supramolecular Structure and Materials of Jilin University.

Supporting Information Available: Cartesian coordinates for studied compounds and **Z2$_H$-G**, energies and symmetries of the frontier molecular orbitals HOMO−4 to LUMO+4, and contour surfaces of the HOMO−1 to LUMO+1 of studied compounds as well as ZINDO/SDCI transition dipole moments between the main electronic states for **1c-Zn**, **2c*-Zn**, **3c-Zn**, **1f-Zn**, **2f-Zn**, and **3f-Zn** are available. This material is available free of charge via the Internet at http://pubs.acs.org.

References and Notes

(1) (a) Bhawalkar, J. D.; He, G. S.; Prasad, P. N. *Rep. Prog. Phys.* **1996**, *59*, 1041. (b) He, G. S.; Zhao, C.-F.; Bhawalkar, J. D.; Prasad, P. N. *Appl. Phys. Lett.* **1995**, *67*, 3703. (c) Zhao, C.-F.; He, G. S.; Bhawalkar, J. D.; Park, C. K.; Prasad, P. N. *Chem. Mater.* **1995**, *7*, 1979.

(2) (a) Fleitz, P. A.; Sutherland, R. A.; Stroghendl, F. P.; Larson, F. P.; Dalton, L. R. *SPIE Proc.* **1998**, *3472*, 91. (b) He, G. S.; Bhawalkar, J. D.; Zhao, C.-F.; Prasad, P. N. *Appl. Phys. Lett.* **1995**, *67*, 2433. (c) Ehrlich, J. E.; Wu, X.-L.; Lee, I.-Y. S.; Hu, Z.-Y.; Röeckel, H.; Marder, S. R.; Perry, J. W. *Opt. Lett.* **1997**, *22*, 1843.

(3) Bhawalkar, J. D.; Kumar, N. D.; Zhao, C.-F.; Prasad, P. N. *J. Clin. Laser Med. Surg.* **1997**, *15*, 201.

(4) (a) Maruo, S.; Nakamura, O.; Kawata, S. *Opt. Lett.* **1997**, *22*, 132. (b) Cumpston, B. H.; Ananthavel, S. P.; Barlow, S.; Dyer, D. L.; Ehrlich, J. E.; Erskine, L. L.; Heikal, A. A.; Kuebler, S. M.; Lee, I.-Y. S.; McCord-Maughon, D.; Qin, J.; Röckel, H. R.; Rumi, M.; Wu, X.-L.; Marder, S. R.; Perry, J. W. *Nature* **1999**, *398*, 51. (c) Kawata, S.; Sun, H.-B.; Tanaka, T.; Takada, K. *Nature* **2001**, *412*, 697. (d) Maruo, S.; Ikuta, K. *Proc. SPIE—Int. Soc. Opt. Eng.* **2000**, *3937*, 106.

(5) Albota, M.; Beljonne, D.; Brédas, J.-L.; Ehrlich, J. E.; Fu, J.-Y.; Heikal, A. A.; Hess, S. E.; Kogej, T.; Levin, M. D.; Marder, S. R.; McCord-Maughon, D.; Perry, J. W.; Röckel, H.; Rumi, M.; Subramaniam, G.; Webb, W. W.; Wu, X.-L.; Xu, C. *Science* **1998**, *281*, 1653.

(6) (a) Reinhardt, B.; Brott, L. L.; Clarson, S. J.; Dillard, A. G.; Bhatt, J. C.; Kannan, R.; Yuan, L.; He, G. S.; Prasad, P. N. *Chem. Mater.* **1998**, *10*, 1863. (b) Kannan, R.; He, G. S.; Yuan, L.; Xu, F.; Prasad, P. N.; Dombroskie, A.; Reinhardt, B. A.; Baur, J. W.; Vaia, R. A.; Tan, L.-S. *Chem. Mater.* **2001**, *13*, 1896. (c) Wang, C.-K.; Macak, P.; Luo, Y.; Agren, H. *J. Chem. Phys.* **2001**, *114*, 9813.

(7) (a) Ventelon, L.; Charier, S.; Moreaux, L.; Mertz, J.; Blanchard-Desce, M. *Angew. Chem.* **2001**, *113*, 2156. *Angew. Chem., Int. Ed.* **2001**, *40*, 2098. (b) Abotto, A.; Beverina, L.; Nozio, R.; Facchetti, A.; Ferrante, C.; Pagani, G. A.; Pedron, D.; Signorini, R. *Org. Lett.* **2002**, *4*, 1495. (c) Strehmel, B.; Sarker, A. M.; Detert, H. *Chem. Phys. Chem.* **2003**, *4*, 249.

(8) (a) Bhawalkar, J. D.; He, G. S.; Park, C.-K.; Zhao, C. F.; Ruland, G.; Prasad, P. N. *Opt. Commun.* **1996**, *124*, 33. (b) He, G. S.; Yuan, L.; Cheng, N.; Bhawalkar, J. D.; Prasad, P. N.; Brott, L. L.; Clarson, S. J.; Reinhardt, B. A. *J. Opt. Soc. Am. B* **1997**, *14*, 1079. (c) He, G. S.; Yuan, L.; Prasad, P. N.; Abotto, A.; Facchetti, A.; Pagani, G. A. *Opt. Commun.* **1997**, *140*, 49. (d) Abotto, A.; Beverina, L.; Bozio, R.; Bradamante, S.; Ferrante, C.; Pagani, G. A.; Signorini, R. *Adv. Mater.* **2000**, *12*, 1963.

(9) (a) Painelli, A.; Del, Freo, L.; Terenziani, F. *Chem. Phys. Lett.* **2001**, *346*, 470. (b) Zalesny, R.; Bartowiak, W.; Styrcz, S.; Leszczynski, J. *J. Phys. Chem. A* **2002**, *106*, 4032. (c) Lei, H.; Huang, Z. L.; Wang, H. Z.; Tang, X. J.; Wu, L. Z.; Zhou, G. Y.; Wang, D.; Tian, Y. B. *Chem. Phys. Lett.* **2002**, *352*, 240.

(10) Kogej, T.; Beljonne, D.; Meyers, F.; Perry, J. W.; Marder, S. R.; Brédas, J.-L. *Chem. Phys. Lett.* **1998**, *298*, 1.

(11) (a) Peticolas, W. L. *Annu. Rev. Phys. Chem.* **1976**, *18*, 233. (b) McClain, W. M. *Acc. Chem. Res.* **1974**, *7*, 129. (c) Birge, R. R.; Pierce, B. M. *J. Chem. Phys.* **1979**, *70*, 165.

(12) (a) Ledoux, I.; Zyss, J.; Siegel, J.; Lehn, J.-M. *Chem. Phys. Lett.* **1990**, *172*, 440. (b) Zyss, J. *Nonlinear Opt.* **1991**, *1*, 3. (c) Zyss, J. *J. Chem. Phys.* **1993**, *98*, 6583. (d) Zyss, J.; Dhenaut, C.; Chau Van, T.; Ledoux, I. *Chem. Phys. Lett.* **1993**, *206*, 409. (e) Zyss, J.; Ledoux, I. *Chem. Rev.* **1994**, *94*, 77.

(13) Burland, D. M. *Chem. Rev.* **1994**, *94*, 1.

(14) (a) Vance, F. W.; Hupp, J. T. *J. Am. Chem. Soc.* **1999**, *121*, 4047. (b) Maury, O.; Le Bozec, H. *Acc. Chem. Res.* **2005**, *38*, 691.

(15) Voigt-Martin, I. G.; Li, G.; Yakimanski, A.; Schulz, G.; Wolff, J. J. *J. Am. Chem. Soc.* **1996**, *118*, 12830.

(16) Bredas, J. L.; Meyers, F.; Pierce, B. M.; Zyss, J. *J. Am. Chem. Soc.* **1992**, *114*, 4928.

(17) (a) Cho, B. R.; Piao, M. J.; Son, K. H.; Lee, S. H.; Yoon, S. J.; Jeon, S.-J.; Cho, M. *Chem. Eur. J.* **2002**, *8*, 3907. (b) Vagin, S.; Barthel, M.; Dini, D.; Michael, A. *Inorg. Chem.* **2003**, *42*, 2683.

(18) (a) Hurst, S. K.; Humphrey, M. G.; Isoshima, T.; Wostyn, K.; Asselberghs, I.; Clays, K.; Persoons, A.; Samoc, M.; Luther-Davices, B. *Organometallics* **2002**, *21*, 2024. (b) Alcaraz, G.; Euzenat, L.; Mongin, O.; Katan, C.; Ledoux, I.; Zyss, J.; Blanchard-Desce, M.; Vaultier, M. *Chem. Commun.* **2003**, 2766. (c) Porrès, L.; Mongin, O.; Katan, C.; Charlot, M.; Pons, T.; Mertz, J.; Blanchard-Desce, M. *Org. Lett.* **2004**, *6*, 47.

(19) (a) Cho, B. C.; Son, K. H.; Lee, S. H.; Song, Y. S.; Lee, Y. K.; Jeon, S. J.; Choi, J. H.; Lee, H.; Cho, M. *J. Am. Chem. Soc.* **2001**, *123*, 10039. (b) Ray, P. C.; Leszczynski, J. *J. Phys. Chem. A* **2005**, *109*, 6689. (c) Kannan, R.; He, G. S.; Lin, T. C.; Prasad, P. N.; Vaia, R. A.; Tan, L.-S. *Chem. Mater.* **2004**, *16*, 185.

(20) (a) Chung, S.-J.; Kim, K.-S.; Lin, T.-Ch.; He, G. S.; Swiatkiewicz, J.; Prasad, P. N. *J. Phys. Chem. B* **1999**, *103*, 10741. (b) Lee, W.-H.; Lee, H.; Kim, J.-A.; Choi, J.-H.; Cho, M.; Jeon, S.-J.; Cho, B. R. *J. Am. Chem. Soc.* **2001**, *123*, 10658. (c) Beljonne, D.; Zojer, E.; Shuai, Z.; Vogel, H.; Wenseleers, W.; Pond, S. J. K.; Perry, J. W.; Marder, S. R.; Bredas, J.-L. *Adv. Funct. Mater.* **2002**, *12*, 631. (d) Macak, P.; Luo, Y.; Norman, P.; Ågren, H. *J. Chem. Phys.* **2000**, *113*, 7055. (e) Chung, S. J.; Lin, T. C.; Kim, K. S.; He, G. S.; Swiatkiewicz, J.; Prasad, P. N.; Baker, G. A.; Bright, F. V. *Chem. Mater.* **2001**, *13*, 4071. (f) Lee, H. J.; Sohn, J. W.; Hwang, J. H.; Park, S. Y. *Chem. Mater.* **2004**, *16*, 456. (g) Liu, X.-J.; Feng, J.-K.; Ren, A.-M.; Cheng, H.; Zhou, X. *J. Chem. Phys.* **2004**, *121*, 8253.

(21) (a) Zhou, X.; Feng, J.-K.; Ren, A.-M. *Chem. Phys. Lett.* **2005**, *403*, 7. (b) Bartholomew, G. P.; Rumi, M.; Pond, S. J. K.; Perry, J. W.; Tretiak, S.; Bazan, G. C. *J. Am. Chem. Soc.* **2004**, *126*, 11529. (c) Zhang, X.-B.; Feng, J.-K.; Ren, A.-M.; Sun, C.-C. *J. Mol. Stru. (THEOCHEM)* **2005**, *756*, 133. (d) Zhou, X.; Ren, A.-M.; Feng, J.-K.; Liu, X.-J. *Chem. Phys. Lett.* **2003**, *373*, 167. (e) Zhang, X.-B.; Feng, J.-K.; Ren, A.-M.; Zhou, X. *Chem. Phys.* **2006**, *322*, 269.

(22) Pond, S. J. K.; Tsutsumi, O.; Rumi, M.; Kwon, O.; Zojer, E.; Brédas, J.-L.; Marder, S. R.; Perry, J. W. *J. Am. Chem. Soc.* **2004**, *126*, 9291.

(23) Zheng, Q.; He, G. S.; Prasad, P. N. J. *Mater. Chem.* **2005**, *15*, 579.

(24) Das, S.; Nag, A.; Goswami, D.; Bharadwaj, P. K. *J. Am. Chem. Soc.* **2006**, *128*, 402.
(25) Renouard, T.; Bozec, H. L.; Brasselet, S.; Ledoux, I.; Zyss, J. *Chem. Commun.* **1999**, 871.
(26) Hilton, A.; Renouard, T.; Maury, O.; Bozec, H. L.; Ledoux, I.; Zyss, J. *Chem. Commun.* **1999**, 2521.
(27) Sénéchal, K.; Maury, O.; Bozec, H. L.; Ledoux, I.; Zyss, J. *J. Am. Chem. Soc.* **2002**, *124*, 4560.
(28) Maury, O.; Viau, L.; Sénéchal, K.; Corre, B.; Guégan, J.-P.; Renouard, T.; Ledoux, I.; Zyss, J.; Bozec, H. L. *Chem. Eur. J.* **2004**, *10*, 4454.
(29) Maury, O.; Bozec, H. L. *Acc. Chem. Res.* **2005**, *38*, 691.
(30) Cha, M.; Torruellas, W. E.; Stegeman, G. I.; Horsthuis, W. H. G.; Möhlmann, G. R.; Meth, J. *Appl. Phys. Lett.* **1994**, *65*, 2648.
(31) Kogej, T.; Beljoone, D.; Meyers, F.; Perry, J. W.; Marder, S. R.; Brédas, J.-L. *Chem. Phys. Lett.* **1998**, *298*, 1.
(32) Orr, B. J.; Ward, J. F. *Mol. Phys.* **1971**, *20*, 513.
(33) Bishop, D. M.; Luis, J. M.; Kirtman, B. *J. Chem. Phys.* **2002**, *116*, 9729.
(34) (a) Anderson, W. P.; Edwards, W. D.; Zerner, M. C. *Inorg. Chem.* **1986**, *25*, 2728. (b) Frisch, M. J.; et al. *Gaussian 03*, revision C.02; Gaussian, Inc.: Wallingford CT, 2004.
(35) Zojer, E.; Kogej, T.; Vogel, H.; Marder, S. R.; Perry, J. W.; Brédas, J. L. *J. Chem. Phys.* **2002**, *116*, 3646.
(36) Ikeda, C.; Yoon, Z. S.; Park, M.; Inoue, H.; Kim, D.; Osuka, A. *J. Am. Chem. Soc.* **2005**, *127*, 534.
(37) Ahn, T. K.; Kim, K. S.; Kim, D. Y.; Noh, S. B.; Aratani, N.; Ikeda, C.; Osuka, A.; Kim, D. *J. Am. Chem. Soc.* **2006**, *128*, 1700.